Inorganic Chemistry

Article

pubs.acs.org/IC

New Multi-Ferrocenyl- and Multi-Ferricenyl- Materials via Coordination-Driven Self-Assembly and via Charge-Driven Electro-Crystallization

Hakikulla H. Shah,[†] Rayya A. Al-Balushi,[†] Mohammed K. Al-Suti,[†] Muhammad S. Khan,*[,†] Christopher H. Woodall,[‡] Anna L. Sudlow,[‡] Paul R. Raithby,*[,‡] Gabriele Kociok-Köhn,[‡] Kieran C. Molloy,*[,‡] and Frank Marken*[,‡]

[†]Department of Chemistry, Sultan Qaboos University, P.O. Box 36, Al-Khodh 123, Sultanate of Oman

[‡]Department of Chemistry, University of Bath, Bath, BA2 7AY, U.K.

Supporting Information

ABSTRACT: Three new tetra-ferrocenylethynylpyridinyl copper complexes, $L_4(CuI)_4$ (**3**), $L_4(CuBr)_2$ (**4**), and $L_4(CuCl)_2$ (**5**) have been prepared from the reaction of ferrocenylethynylpyridine (L)(**2**) with copper halides CuX (with X = I^-, Br^-, Cl^-).The ligand **2** and the complexes **3**−**5** have been fully characterized by spectroscopic methods. The structures of **2**−**4** have been confirmed by single-crystal X-ray crystallography. **2** forms a dimer in the crystalline-state through C−H··N hydrogen bonds. **4** and **5** are dimers and **3** a tetramer, in all cases linked through Cu−X··Cu bridging interactions. Cyclic voltammetry in dichloroethane showed chemically reversible multiferrocenyl oxidation signals with evidence for product electrocrystallization. The oxidation products were isolated by electrodeposition onto a Pt disc electrode and investigated by scanning electron microscopy which confirmed the spontaneous formation of crystalline oxidation products with distinctive morphologies. Energy dispersive X-ray elemental analysis shows the presence of hexafluorophosphate (counterion) with the P:Fe ratio of 1:1, 0.5:1, and 1:1 for the electrocrystallized products **3**, **4**, and **5**, respectively, suggesting the formulas $[\mathbf{3}]^{4+}(PF_6^-)_4$, $[\mathbf{4}]^{2+}(PF_6^-)_2$, and $[\mathbf{5}]^{4+}(PF_6^-)_4$ for the electrocrystallized products.

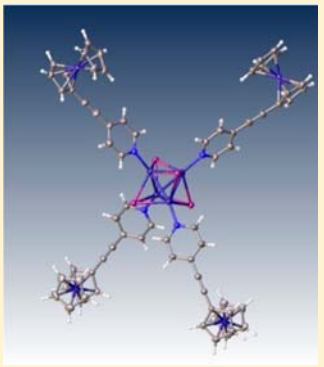

INTRODUCTION

Copper(I) is known for its ability to form multinuclear (cluster) species of various shapes and sizes, on reaction with a range of bridging and terminal ligands, where weak bonding interactions between the closed-shell metal centers are generally present.[1−5] Clusters based on rhomboid $(CuX)_2$ dimers,[4,6−8]cubane$(CuX)_4$ tetramers,[8−10] infinite $(CuX)_\infty$ zigzag,[11−14] or stair-step polymers[11,12](X= halide) have been investigated by many research groups for their rich photophysical properties. Particularly, the $(CuX)_4(Py\text{-}x)_4$ series (where Py-x is a substituted pyridine) have been the subject of the majority of quantitative photophysical studies.[15−19] We have a long-standing interest in organometallic oligomers and polymers linked by alkynes for opto-electronic applications.[20−31] Following reports of mixed-valence stabilization in ferrocenyl-terminated redox star complexes[32] our recent studies on *bis*-ferrocenylethynyl complexes incorporating conjugated heterocyclic spacers,[33] we now turn our attention to show how the copper clusters can be utilized to produce tetra-ferrocenyl mixed-valence materials. At the molecular level the building-block for the quantum-dot cellular automata is a symmetric mixed-valence complex in which the binary states 0 or 1 are represented by the location of a mobile electron (or a hole) at one of the two metal centers.[34] However, arrays with four redox sites are generally considered more versatile and efficient cell designs for use in logic applications.[35,36] Functionalization of the (Py-x) to ferrocenylethynyl-pyridine in $(CuX)_4(Py\text{-}x)_4$ series gives easy and straightforward access to these remarkable series of tetra-ferrocenyl copper complexes possessing fascinating structures and electrochemical properties. Several strategies for rational syntheses of complexes with four redox sites have been reported. These often require considerable synthetic effort to prepare and can be plagued by low yields and largely amorphous final structures. When issues such as functional group, structural precision, synthetic ease, and building-block versatility come into question, coordination-driven self-assembly may provide a powerful alternative to the purely covalent synthesis of multifunctional molecules.[37]

Herein, we report the synthesis of three new tetra-(ferrocenylethynyl-pyridinyl)copper complexes formed by the coordination-driven self-assembly of the ferrocenylethynyl-pyridine ligand (L) (**2**) and the copper(I) halides (I^-, Br^-, Cl^-), forming cubic $L_4(CuI)_4$ (**3**), rhomboid $L_4(CuBr)_2$ (**4**), and $L_4(CuCl)_2$ (**5**) complexes. Complete characterization using spectroscopic and electrochemical techniques has been carried out. Structures of **2**−**4** have been confirmed by X-ray crystallography. During the cyclic voltammetry of complexes **3**−**5**, a "stripping reduction peak" evident of electrocrystallization of the oxidation products was observed. The

Received: July 12, 2013
Published: October 9, 2013

dx.doi.org/10.1021/ic401803p | *Inorg. Chem.* 2013, 52, 12012−12022

Table 1. Crystallographic Data for 2−4

	2	3	4
empirical formula	$C_{17}H_{13}FeN$	$C_{35}H_{27}Cl_3Cu_2Fe_2I_2N_2$	$C_{68.3}H_{52.6}Br_2Cl_{0.6}Cu_2Fe_4N_4$
formula weight	287.13	1074.52	1460.91
crystal system	Monoclinic	Monoclinic	Triclinic
space group	$P2_1/c$	$C2/c$	$P\bar{1}$
a	11.872(5)	25.2705(7)	9.8408(2)
b	10.065(5)	9.8792(2)	13.3736(3)
c	10.672(5)	31.8663(8)	23.7742(5)
α			105.158(1)
β	92.335(5)	111.970(3)	92.748(1)
γ			94.484(1)
V (Å^3)	1274.2(10)	7377.8(3)	3003.13(11)
T (K)	150(2)	150(2)	150(2)
Z	4	8	2
ρ_{calc} Mg m^{-3}	1.497	1.935	1.616
μ(Mo-K_α) (mm^{-1})	1.166	3.827	3.038
F(000)	592	4144	1465
crystal size (mm)	0.30 × 0.10 × 0.10	0.20 × 0.10 × 0.05	0.30 × 0.20 × 0.05
θ range (deg)	2.78 to 29.57.	2.79 to 29.67.	2.93 to 25.00
reflections collected	22131	36127	40103
independent refl'ns [R(int)]	3247 [0.0293]	9262 [0.0414]	10242 [0.0630]
reflections observed (>2σ)	2718	6818	8417
max. and min transmission	0.8923, 0.7212	0.8317, 0.5149	0.8629, 0.4626
goodness-of-fit on F^2	1.038	1.011	1.021
final R_1, wR_2 [$I > 2\sigma(I)$]	0.0447, 0.1148	0.0384, 0.0692	0.0953,0.2737
final R_1, wR_2 (all data)	0.0560, 0.1224	0.0663, 0.0769	0.1129, 0.2938
largest diff. peak, hole (e Å^3)	1.728, −0.489	1.230, −1.202	5.000, −1.936

oxidation products were electrodeposited onto the electrode surface and isolated for investigation by scanning electron microscopy (SEM) which showed distinct morphological arrangements for the electro-crystallized products such as dendritic for $[\mathbf{3}]^{4+}[PF_6^-]_4$ while "lettuce" or "flower-like" for $[\mathbf{4}]^{2+}[PF_6^-]_2$ and $[\mathbf{5}]^{4+}[PF_6^-]_4$ (molecular structures assigned here tentatively, vide infra). Raman spectroscopy and energy dispersive X-ray (EDX) elemental analysis showed the presence of a $[PF_6]^-$ (counterion) and a P:Fe ratio of 1:1, 0.5:1 and 1:1 suggesting partially- and fully oxidized materials and cocrystallization of $[PF_6]^-$ with the formulas $[\mathbf{3}]^{4+}[PF_6^-]_4$, $[\mathbf{4}]^{2+}[PF_6^-]_2$, and $[\mathbf{5}]^{4+}[PF_6^-]_4$, respectively, for the electrocrystallized products. A recently identified family of ferroelectric structures is based on intermolecular charge transfer crystals,[38] where donor (tetrathiafulvalene) and acceptor (*p*-chloranil) molecules cocrystallize in an alternating fashion known as mixed stack.[39] In the crystal lattice a collective transfer of electrons from donor to acceptor molecules results in dipole formation that can be realigned by the application of external field as molecules switch partners in the mixed stack. The crystalline $[\mathbf{3}]^{4+}[PF_6^-]_4$, $[\mathbf{4}]^{2+}[PF_6^-]_2$, and $[\mathbf{5}]^{4+}[PF_6^-]_4$ materials could be an entry to such ferroelectric materials.[40−42] The dendritic and the "flower-like" morphologies of the electrodeposited Cu-based microstructure are of high recent interest for fundamental studies and for potential applications in catalysis and other fields.[43−46]

EXPERIMENTAL SECTION

All reactions were carried out under inert atmosphere using Schlenk techniques. Solvents were predried and distilled from appropriate drying agents. All chemicals, unless otherwise stated, were obtained from commercial sources and used as received. The key starting material, ethynylferrocene (**1**), was synthesized by an adaptation of a literature method.[47] ^{1}H NMR spectra were recorded on a Bruker AM-400 spectrometer in $CDCl_3$ and were referenced to solvent resonances. IR spectra were recorded as CH_2Cl_2 solutions in a NaCl cell on a Nicolet-Impact 400D FT-IR spectrometer. Mass spectra were obtained on a Kratos MS 890 spectrometer by the electron impact (EI) and fast atom bombardment (FAB) techniques. Microanalyses were performed in the Department of Chemistry, University of Bath, U.K. Column chromatography was performed either on Kieselgel 60 (230−400 mesh) silica gel or alumina (Brockman grade II−III).

Scanning Electron Microscopy (SEM) and Electron Dispersive X-ray Analysis (EDX). Solid samples were fixed to carbon tape which was mounted onto conductive SEM stubs. Electrodes were mounted in a special holder and earthed to avoid charging of the surface. SEM images were taken either on a JEOL JSM 6480LV Scanning Electron Microscope using a BSE detector and an accelerating voltage of 15 kV or on a JEOL JSM 6301F Field Emission Scanning Electron Microscope using an SEI detector and an accelerating voltage of 5 kV. EDX measurements were taken on a JEOL JSM 6480LV Scanning Electron Microscope using an accelerating voltage of 15 kV.

Raman Spectroscopy. Raman spectra were recorded on a Renishaw inVia Raman Microscope using a solid-state laser with an excitation wavelength of 532 nm and a power of 2.5 mW. Spectra were taken directly from the electrode surface using a 20× objective to focus on the crystals. Spectra of the solid samples were taken using the same objective; samples were mounted on either a glass slide or on carbon tape.

Electrochemistry. Cyclic voltammograms were recorded in a dried glass cell purged under purified argon. A 3 mm diameter platinum disc electrode was used as working electrode and a Pt-wire served as counter electrode, while a KCl-saturated calomel electrode (SCE, Radiometer ref 401) served as the reference electrode. Electrolyte solutions were prepared from dichloroethane (DCE) and $[n\text{-}Bu_4N^+][PF_6^-]$ (0.1 M, Fluka, dried in oil-pump vacuum) as supporting electrolyte. The respective organometallic complexes were added at about 1 mM concentration. Cyclic voltammograms were recorded using a micro Autolab III (Ecochemie, The Netherlands).

Synthesis. *Ferrocenylethynyl-pyridine (L) (**2**).* Ethynylferrocene (**1**)[47] (0.33 g, 1.51 mmol) and 4-iodopyridine (0.31 g, 1.5 mmol) were dissolved in diisopropylamine:tetrahydrofuran mixture (1:5) (60 mL)-under an argon atmosphere. Catalytic amounts of $Pd(OAc)_2$ (3 mg), CuI

dx.doi.org/10.1021/ic401803p | *Inorg. Chem.* 2013, 52, 12012−12022

Scheme 1. Synthesis of Compound 2

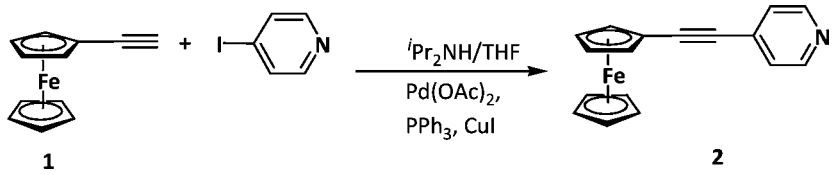

Scheme 2. Synthesis of Complexes 3−5

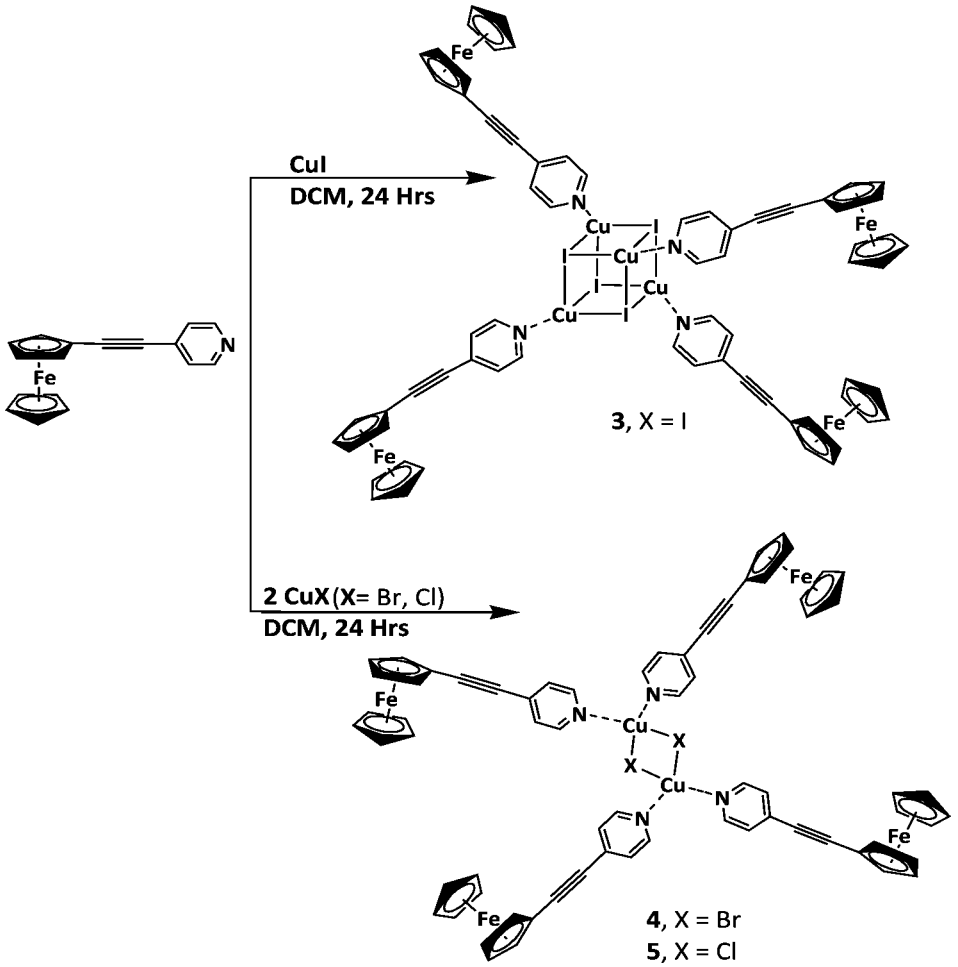

(3 mg), and PPh_3 (10 mg) were added to the reaction mixture, which was left under reflux for 24 h after which all volatile components were removed under reduced pressure. The residue was dissolved in dichloromethane (100 mL) and washed with water in a separating funnel. The aqueous layer was extracted three times with dichloromethane (20 mL). The combined organic layer was washed with water and brine and then dried over anhydrous magnesium sulfate. The solution was concentrated under vacuum, and the crude product was flash chromatographed through a silica column using hexane: dichloromethane (1:1, v/v) as eluent to obtain the complex as an orange crystalline product (0.35 g, 81% yield). IR (CH_2Cl_2, cm^{-1}): 2210ν(C≡C), 416 ν($Ring_{Pyr}$), 1454 ν(C=N_{Pyr}), 1025 ν(CCH_{pyr}) and 484 ν(FeCp). ^{1}H NMR ($CDCl_3$): δ (ppm) 4.26 (s, 5H, Cp), 4.30 (pseudo-t, 2H, Cp), 4.54 (pseudo-t, 2H, Cp), 7.33 (d, J = 6.0 Hz, 2H, $H_{\beta\text{-pyr}}$), 8.56 (d, J = 6.0 Hz, 2H, $H_{\alpha\text{-pyr}}$). FABMS: m/z 288 (M^+)$C_{17}H_{13}$FeN: Analysis, calc. C, 71.11; H, 4.56%; found: C, 71.18; H, 4.49%.

*$L_4(CuI)_4$ (**3**)[L = **2**].* Ferrocenylethynyl-pyridine (**2**) (0.040 g, 0.14 mmol) and CuI (0.027 g, 0.14 mmol) were dissolved in dry dichloromethane (20 mL) and allowed to stir at room temperature under argon for 24 h. The crude product obtained after removal of the solvent under reduced pressure was redissolved in CH_2Cl_2 and filtered through a pad of Celite using CH_2Cl_2 giving orange micro crystals (0.048 g, 72% yield). IR ($CH_2Cl_2cm^{-1}$): 2208 ν(C≡C), 433 ν(Ring $_{Pyr}$), 1452 ν(C=N_{Pyr}), 1014 ν(CCH_{pyr}), and 472 ν(FeCp).^{1}H NMR ($CDCl_3$): δ (ppm) 4.27 (s, 20H, Cp), 4.33 (pseudo-t, 8H, Cp), 4.57 (pseudo-t, 8H, Cp), 7.49 (d, 8H, J = 7.5 Hz, $H_{\beta\text{-pyr}}$), 7.67 (d, 8H, J = 11.7 Hz, $H_{\alpha\text{-pyr}}$). FABMS: m/z 1911 (M^+). $C_{68}H_{52}Cu_4Fe_4I_4N_4$: Analysis, calc.: C, 42.75; H, 2.74%;found: C, 42.78; H, 2.79%.

*$L_4(CuBr)_2$ (**4**).* The title compound was synthesized by following a procedure similar to that described above for **3** using **2** (0.080 g, 0.28 mmol) and CuBr (0.020 g, 0.14 mmol). The crude product obtained after removal of the solvent under reduced pressure was redissolved in CH_2Cl_2 and filtered through a pad of Celite using CH_2Cl_2 giving orange micro crystals (0.038 g, 63% yield). IR ($CH_2Cl_2cm^{-1}$): 2207 ν(C≡C), 435 ν(Ring $_{Pyr}$), 1454 ν(C=N_{Pyr}), 1027 ν(CCH_{pyr}), and 472 ν(FeCp). ^{1}H NMR ($CDCl_3$): δ(ppm) 4.26 (s, 20H, Cp), 4.31 (pseudo-t, 8H, Cp), 4.55 (pseudo-t, 8H, Cp), 7.49 (d, 8H, J = 7.5 Hz,$H_{\beta\text{-pyr}}$), 7.69 (d, 8H, J = 12.1 Hz, $H_{\alpha\text{-pyr}}$). FABMS: m/z 1436 (M^+). $C_{68}H_{52}Br_2Cu_2Fe_4N_4$: Analysis, calc.: C, 56.90; H, 3.65%; found: C, 56.96; H, 3.61%.

*$L_4(CuCl)_2$ (**5**).* The compound was synthesized by following a procedure similar to that described above for **3** using **2** (0.080 g, 0.28 mmol) and CuCl (0.014 g, 0.14 mmol). The crude product obtained

dx.doi.org/10.1021/ic401803p | *Inorg. Chem.* 2013, 52, 12012−12022

Table 2. Raman Vibrational Frequencies (cm^{-1}) of Ligand 2, Complexes 3−5, and Electrocrystallized Products $[3]^{4+}[PF_6^-]_4$, $[4]^{2+}[PF_6^-]_2$, and $[5]^{4+}[PF_6^-]_4$[a]

2	3	4	5	$[3]^{4+}[PF_6^-]_4$	$[4]^{2+}[PF_6^-]_2$	$[5]^{4+}[PF_6^-]_4$	assignment
	295	301	301	293	301	292	Cu−X [X = I(3), Br(4), Cl(5)]
	328	417	418	324	396	389	Cu−N
986	1012	1022	1022	1014	1025	1030	CNC (Py)
1172	1171	1174	1172	1175	1172	1176	Fc
1593	1598	1608	1606	1602	1609	1613	CN (Py)
2208	2203	2206	2203	2206[a]	2206[b]	2206[a]	C≡C

[a]All Raman intensities are in arbitrary units. [b]Broad split peak.

Table 3. UV-vis Spectral Data for 2 and Complexes 3−5 in Dichloromethane

compound	wavelength (λ_{max} / nm)
2 [L]	255, 308, 350, 455
3 $[L_4(CuI)_4]$	255, 308, 375, 464
4 $[L_4(CuBr)_2]$	257, 307, 377, 478
5 $[L_4(CuCl)_2]$	265, 309, 381, 480

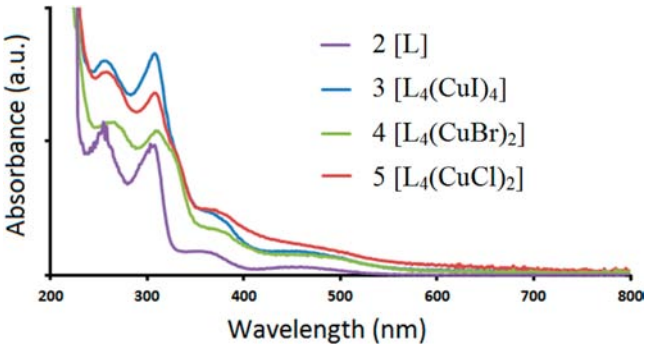

Figure 1. UV−vis spectra for complexes **2**−**5** in dichloromethane.

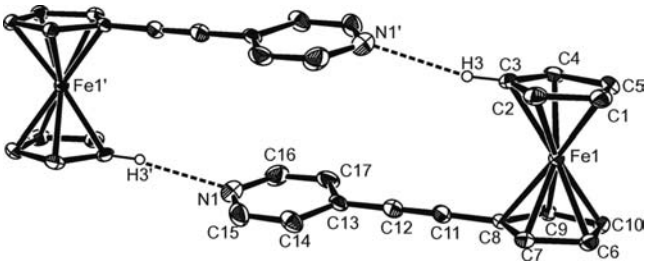

Figure 2. Structure of **2** showing the asymmetric unit and the labeling scheme used in the text; thermal ellipsoids are at the 30% level. Only H(3) of the hydrogen atoms, which is the one involved in hydrogen bonding, is shown for clarity. Selected geometric data: Fe(1)−C(1,5) ring centroid 1.6507(13), Fe(1)−C(6,10) ring centroid 1.6473(12), C(8)−C(11) 1.415(4), C(11)−C(12) 1.209(4), C(12)−C(13) 1.378(4), C(15)−N(1) 1.358(5), C(16)−N(1) 1.338(5) Å; C(12)−C(11)−C(8) 178.5(3), C(11)−C(12)−C(13) 179.3(3)°. H-bond data: H(3)··N(1): 2.588(3) Å; ∠C(3)−H(3)···N(1): 169.34(17)°. Symmetry operation: −*x*, 1−*y*, 1−*z*.

after removal of the solvent under reduced pressure was redissolved in CH_2Cl_2 and filtered through a pad of Celite using CH_2Cl_2 giving orange micro crystals (0.056 g, 51% yield). IR (CH_2Cl_2 cm^{-1}): 2206 ν(C≡C), 430 ν(Ring $_{Pyr}$), 1458 ν(C═N_{Pyr}), 1028 ν(CCH_{pyr}), and 472 ν(FeCp). ^{1}H NMR ($CDCl_3$): δ(ppm) 4.27 (s, 20H, Cp), 4.31 (pseudo-t, 8H, Cp), 4.55 (pseudo-t, 8H, Cp), 7.49 (d, 5H, J = 7.5 Hz, $H_{\beta\text{-pyr}}$), 7.67 (d, 1H, J = 12.1 Hz, $H_{\alpha\text{-pyr}}$). FABMS: m/z: 1347. $C_{68}H_{52}Cl_2Cu_2Fe_4N_4$: Analysis, calc.: C, 60.65; H, 3.89%; found: C, 60.78; H, 3.79%.

X-ray Crystallography. Single-crystal X-ray diffraction experiments were performed at 150(2) K on either an Oxford Diffraction Gemini A Ultra CCD diffractometer (**2**, **3**) or an Nonius Kappa CCD diffractometer (**4**) using monochromatic MoK_α radiation (λ = 0.71073 Å). For **2** and **3** the sample temperature was controlled using an Oxford Diffraction Cryojet apparatus; CrysAlis Pro was used for the collection of frames of data, indexing reflections, and determining lattice parameters. For **4**, temperature control was achieved using an Oxford

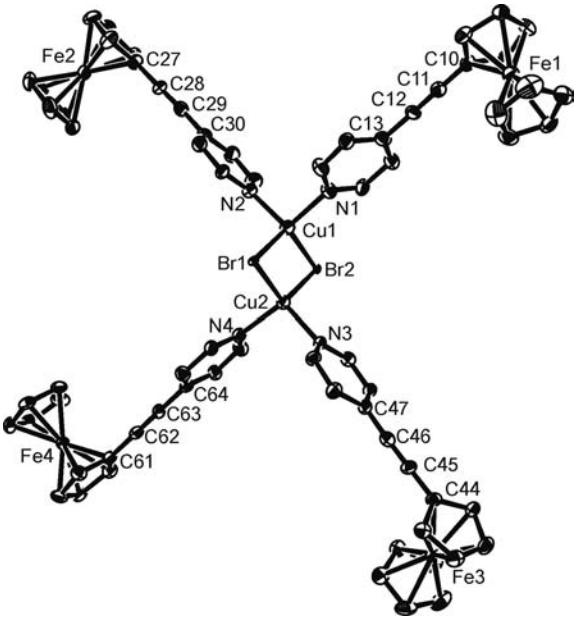

Figure 3. Structure of **4** showing the asymmetric unit and the labeling scheme used in the text; thermal ellipsoids are at the 30% level. Cu(1)−N(1) 2.066(11), Cu(1)−N(2) 2.058(11), Cu(2)−N(3) 2.054(10), Cu(2)−N(4) 2.076(10), Cu(1)−Br(1) 2.6368(18), Cu(1)−Br(2) 2.6138(17), Cu(2)−Br(1) 2.6199(16), Cu(2)−Br(2) 2.6186(16), C(10)−C(11) 1.381(18), C(11)−C(12) 1.229(18), C(12)−C(13) 1.462(17), C(27)−C(28) 1.436(17), C(28)−C(29) 1.232(17), C(29)−C(30) 1.405(18), C(44)−C(45) 1.414(17), C(45)−C(46) 1.234(18), C(46)−C(47) 1.396(18), C(61)−C(62) 1.418(17), C(62)−C(63) 1.205(17), C(63)−C(64) 1.451(16), Fe(1)−C(1,5) ring centroid 1.671(8), Fe(1)−C(6,10) ring centroid 1.654(7), Fe(2)−C(18,22) ring centroid 1.664(7), Fe(2)−C(23,270) ring centroid 1.652(7), Fe(3)−C(35,39) ring centroid 1.644(7), Fe(3)−C(40,44) ring centroid 1.662(7), Fe(4)−C(52,56) ring centroid 1.675(7), Fe(4)−C(57,61) ring centroid 1.634(6)Å; N(1)−Cu(1)−N(2) 101.9(4), N(1)−Cu(1)−Br(1) 106.7(3), N(1)−Cu(1)−Br(2) 109.9(3), N(2)−Cu(1)−Br(1) 109.2(3), N(2)−Cu(1)−Br(2) 107.9(3), Br(1)−Cu(1)−Br(2) 119.83(6), N(3)−Cu(2)−N(4) 103.8(4), N(3)−Cu(2)−Br(1) 107.2(3), N(3)−Cu(2)−Br(2) 110.4(3), N(4)−Cu(2)−Br(1) 106.1(3), N(4)−Cu(2)−Br(2) 107.7(3), Br(2)−Cu(2)−Br(1) 120.29(6), C(10)−C(11)−C(12)-177.9(15), C(11)−C(12)−C(13) 178.8(14), C(27)−C(28)−C(29) 177.6(14), C(28)−C(29)−C(30) 177.2(13), C(44)−C(45)−C(46) 179.0(13), C(45)−C(46)−C(47) 177.6(14), C(61)−C(62)−C(63) 178.4(16), C(62)−C(63)−C(64) 179.4(13)°.

dx.doi.org/10.1021/ic401803p | *Inorg. Chem.* 2013, 52, 12012−12022

Table 4. Comparative Fc-C≡C−C and N:→Cu Geometric Data for 2−4

	C≡C (Å)	Fe−C(≡C) (Å)	(C≡)C−C(py) (Å)	∠Fe−C≡C−C (deg)	N:→Cu (Å)	Cu−X (Å)[a]
Fc-C≡C−C≡C-Fc[b]	1.201(3)	1.428(3)	1.374(4)	178.7(2), 179.8(3)		
2	1.209(4)	1.415(4)	1.378(4)	178.5(3), 179.3(3)		
3	1.193(6)	1.434(6)	1.425(6)	178.7(5), 178.0(6)	2.033(3)	2.6797(6), 2,6955(6), 2.7158(6)
	1.192(6)	1.417(6)	1.427(6)	178.0(4), 175.0(5)	2.021(3)	2.6199(6), 2.6663(6), 2.7850(6)
4	1.229(18)	1.381(18)	1.462(17)	177.9(15), 178.8(14)	2.066(11)	2.6368(18), 2.6138(17)
	1.232(17)	1.436(17)	1.405(18)	177.6(14), 177.2(13)	2.058(11)	2.6199(16), 2.6186(16)
	1.234(18)	1.414(17)	1.396(18)	179.0(13), 177.6(14)	2.054(10)	
	1.205(17)	1.418(17)	1.451(16)	178.4(16), 179.4(13)	2.076(10)	
$[CuBr(2\text{-}MeC_5H_4N)_2]_2$[c]					2.027(7)	2.581(2), 2.607(2)
					2.030(6)	
$[CuI(2\text{-}MeC_5H_4N)_2]_2$[d]					2.05(1)	2.714(3), 2.663(3)
					2.06(1)	
$[(BzMe_2N)CuI]_4$[e]					2.107(3) −2.122(3)	2.6328(7)−2.7121 (6)
$[(Fc')Ph_2P)CuI]_4$[f,g]					2.250(2)−2.255(2)[h]	2.6341(7)−2.7503(7)

[a]X = appropriate halogen, specifically Br (**4**), I (**3**). [b]Ref 33. [c]Ref 65. [d]Ref 66. [e]Ref 67. [f]Ref 68. [g]Fc′ = $[(CH_2{=}CH)C_5H_4]Fe(C_5H_4)$. [h]X = P.

Cryostream device. Structures were solved by direct methods using SHELXS-86[48] and refined by full-matrix least-squares on F^2 using SHELX-97.[49] A multiscan absorption correction was applied in all cases. Crystallographic data for all complexes studied can be found in Table 1. In the case of **3**, there appear to be traces of hexane as well as CH_2Cl_2in the same lattice void though it was not possible to model the hexane component. The molecule of CH_2Cl_2 is itself disordered around a center of inversion with an occupation factor of 30% in total.

RESULTS AND DISCUSSION

Synthesis and Spectroscopic Characterization. A cross-coupling reaction between ethynyl-ferrocene and 4-iodo-pyridine in 1:1 stoichiometry in refluxing $^{i}Pr_2NH$:THF (1:5) mixture readily gave compound **2** (Scheme 1). The crude product was purified by flash chromatography using silica and an orange, crystalline product was obtained in 81% yield.[50]

Compound **2** was used as ligand for the synthesis of complexes **3**−**5** (Scheme 2). For complex **3**, ligand **2** and CuI were reacted in a 1:1 ratio in dry CH_2Cl_2 under argon for 24 h. The product was formed with the ligand coordinating through the pyridyl moiety to each Cu in the CuI cuboids (Scheme 2). However, analogous 1:1 reactions between **2** and other Cu−X (X = Br^-,Cl^-) yielded complexes **4**, **5** incorporating 2:1 ratio of ligand: CuX, where two molecules of the ligand coordinate to a single metal in a dimeric Cu-halide rhomboid via the pyridine functionality (Scheme 2). The ligand **2** and the complexes **3**−**5** are stable to light and air at ambient temperature and were fully characterized by IR, UV, Raman, and NMR spectroscopy, FAB mass spectrometry, as well as by satisfactory elemental analysis.

The IR spectra of the ligand **2** and the complexes **3**−**5** show a single sharp band around 2210 cm^{-1} characteristic of ν(C≡C) in ethynylferrocenyls bonded to aromatic and heteroaromatic groups.[33,51−53] The ν(CpFc) ring vibration signals changed significantly from ligand **2** (484 cm^{-1}) to complexes **3**−**5** (472 cm^{-1}), but among the complexes **3**−**5**, this vibration band is independent of the number of ligands coordinated to each Cu center.[54−56] The pyridine vibrational modes ν(ring), ν(CCH), and ν(C═N) are affected on coordination of the pyridyl ligand to Cu yielding complexes **3**−**5**.[54,55] The pyridine ν(CCH) vibrational band shows a lower value (1014 cm^{-1}) in complex **3** compared to **2** (1025 cm^{-1}), and **4** and **5** (1027 and 1028 cm^{-1}, respectively).

There are also significant shifts in the Raman bands of ligand **2** on coordination to Cu-halides (Table 2). Cu−N and Cu−halide stretching vibrations in the region 200−600 cm^{-1} have been reported for Cu-Pyridine complexes.[57,58] However, for complexes **3**−**5**, two distinct patterns in the Cu−N and Cu-halide bands were observed. For example, the Cu−N stretching vibrations for complexes **3**, **4**, and**5** are observed at 328, 417, and 418 cm^{-1}, respectively, while the Cu−halide stretching vibrations are observed at 295, 301, and 301 cm^{-1}, respectively. The CNC bending vibrations and the CN stretching vibration bands are positively shifted in **3**, and these bands are further positively shifted in complexes **4** and **5** compared to that in **2**. The C≡C band and the ferrocenyl ring breathing modes[59−61] are observed as expected for **2** and experience no significant shifts on complex formation with the Cu-halides, because of the large distance between the terminal ethynyferrocenes and the Cu-coordination center. Overall, bands in complexes **4** and **5** are similar because of the same L:Cu (2:1) stoichiometry and molecular symmetry and are distinctly different from those in complex **3** where the L:Cu stoichiometry is 1:1.

The Raman data for the electro-crystallized complexes $[\mathbf{3}]^{4+}[PF_6^-]_4$, $[\mathbf{4}]^{2+}[PF_6^-]_2$, and $[\mathbf{5}]^{4+}[PF_6^-]_4$ are distinct from those of the parent neutral complexes **3**−**5**. Two patterns are seen in the Raman data for the electro-crystallized complexes. The first arises from the ligand:CuX stoichiometry [1:1 (**3**) and 2:1 (**4** and **5**)] and the second is attributed to the extent of oxidation [half $[\mathbf{4}]^{2+}[PF_6^-]_2$ and full $[\mathbf{3}]^{4+}[PF_6^-]_4$, and $[\mathbf{5}]^{4+}[PF_6^-]_4$]. The electro-crystallized products of the complexes **3**−**5** show stoichiometry-driven Raman shifts similar to those of the IR bands. This can be clearly seen if any effect of oxidation is eliminated. Therefore, we can compare the Raman data between the two fully oxidized species, $[\mathbf{3}]^{4+}[PF_6^-]_4$ and $[\mathbf{5}]^{4+}[PF_6^-]_4$, and the parent complexes **3** and **5** (Table 2). The Fc breathing modes show slight relaxation or positive shifts in the fully oxidized species $[\mathbf{3}]^{4+}[PF_6^-]_4$ and $[\mathbf{5}]^{4+}[PF_6^-]_4$, and a combined effect of these four terminal ferrocenes leads to a contraction of the Cu−N and Cu−X vibrations. The degree of contraction is proportional to and in agreement with the L:Cu stoichiometry. The effect of oxidation can be seen if any effect of stoichiometry is eliminated. Therefore, a comparison of the Raman shifts of the electro-crystallized species $[\mathbf{4}]^{2+}[PF_6^-]_2$ and $[\mathbf{5}]^{4+}[PF_6^-]_4$ with that of the parent complexes **4** and **5**,

dx.doi.org/10.1021/ic401803p | Inorg. Chem. 2013, 52, 12012−12022

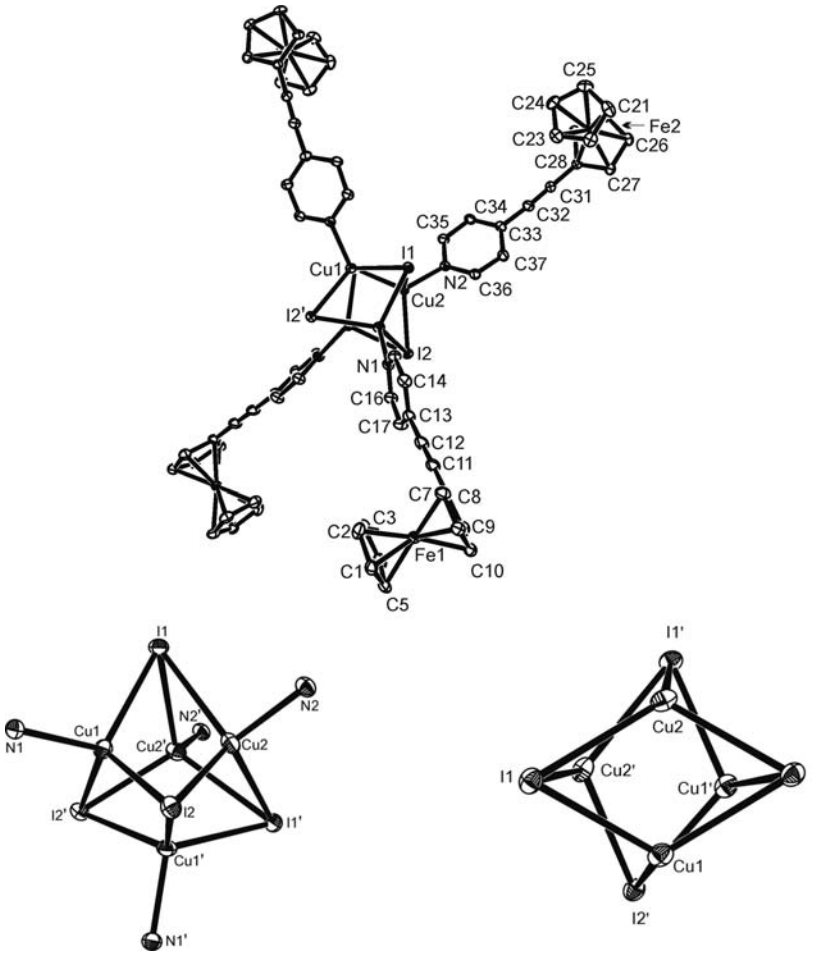

Figure 4. (a) top, (b) bottom left, (c) bottom right. The structure of **3** showing (a) the asymmetric unit and the labeling scheme used in the text; thermal ellipsoids are at the 30% level, and (b) the Cu_4I_4 core. A CH_2Cl_2 molecule of solvation has been omitted for clarity. Selected geometric data: Cu(1)−N(1) 2.033(3), Cu(1)−I(1) 2.6797(6), Cu (1)−I(2′) 2.6955(6), Cu(1)−I(2) 2.7158(6), Cu(2)−N(2) 2.021(3), Cu(2)−I(2) 2.6199(6), Cu(2)−I(1′) 2.6663(6), Cu(2)−I(1) 2.7850(6),: Fe(1)−C(1,5) ring centroid 1.652(3), Fe(1)−C(6,10) ring centroid 1.6442(2), Fe(2)−C(21,25) ring centroid 1.644(2), Fe(2)−C(26,30) ring centroid 1.641(2), C(8)−C(11) 1.434(6), C(11)−C(12) 1.193(6), C(12)−C(13) 1.425(6), C(28)−C(31) 1.417(6), C(31)−C(32) 1.192(6), C(32)−C(33) 1.427(6) Å; N(1)−Cu(1)−I(1) 111.28(10), N(1)−Cu(1)−I(2′) 105.84(10), I(1)−Cu(1)−I(2′) 106.41(2), N(1)−Cu(1)−I(2) 101.71(10), I(1)−Cu(1)−I(2) 111.33(2), I(2)−Cu(1)−I(2′) 120.02(2), N(2)−Cu(2)−I(2) 113.33(10), N(2)−Cu(2)−I(1′) 107.26(10), I(2)−Cu(2)−I(1′) 109.03(2), N(2)−Cu(2)−I(1) 95.47(10), I(2)−Cu(2)−I(1) 111.00(2), I(1)−Cu(2)−I(1′) 120.15(2), C(12)−C(11)−C(8) 178.7(5), C(11)−C(12)−C(13) 178.0(6), C(32)−C(31)−C(28) 178.0(4), C(31)−C(32)−C(33) 175.0(5)°. Symmetry operation: $1 - x, y, {}^1/_2 + z$.

respectively, can be made. The magnitude of the shifts is again proportional to, and in agreement with, the extent of the oxidation (see Table 3). Therefore, these shifts can be attributed to the half- and full-oxidation of complexes **4** and **5**, respectively. Thus, the Raman data confirms the formation of the complexes and supports the proposed hypothesis concerning the half- and full-oxidized forms of the electro-crystallized products. The Raman data also complements the IR results concerning the band shifts due to ligand:Cu stoichiometry.

The ^{1}H NMR spectra showed a pattern of singlet and pseudo triplet, that is, overlapping dd signals at ∼4 ppm for the unsubstituted C_5H_5 and substituted C_5H_4 ferrocenyl Cp protons, respectively. Pyridinyl (C_5H_4N) proton signals were observed in the 7−9 ppm region as doublets.[61] Substantial shifts in the pyridinyl H_α proton of **2** and complex **3**−**5** can be seen, whereby these protons in **3**−**5** are shifted upfield compared to those in **2** on electron donation to Cu upon coordination. Furthermore, among complexes **3**−**5**, a slight increase in the pyridinyl-H_α *J*-coupling value is observed particularly for complexes **4** and **5**. The mass spectra (+ve FAB) displayed the presence of molecular ions with characteristic fragmentation patterns for the complexes **2**−**5**.

The electronic absorption spectra of **2** and the complexes **3**−**5** were recorded in CH_2Cl_2 (Figure 1, Table 3). Each compound displays two sets of absorption bands reminiscent of other ferrocenyl species.[63] Bands with λ_{max} below 400 nm can be attributed to a $\pi-\pi^*$ transition associated with the pyridine group,[62] while a weak absorption band at ∼450 to ∼480 nm is assigned to an Fe^{II} d-d transition.[64]

Structural Characterization. The structures of **2** and the complexes **3**−**4** were confirmed by single-crystal X-ray crystallography. The structure of the ligand, Fc-C≡C-py (**2**) [Fc = $(C_5H_5)Fe(C_5H_4)$; py = 4-NC_5H_4] is shown in Figure 2; selected geometric data are given in the caption. The alkyne links Fc and py fragments in a linear fashion with bond angles at the sp carbons close to 180°, and with a C≡C length [1.209(4) Å] which is at the long end of the range associated with such bonds when measured crystallographically.[33] In addition, both the Fc-C(≡C) and (C≡)C−C bonds show some multiple-bond character (Table 4) and the C−C(py) bond is the shortest bond

dx.doi.org/10.1021/ic401803p | *Inorg. Chem.* 2013, 52, 12012−12022

Table 5. Electrochemical Potential Data in mV vs. SCE for Ligand 2 and Complexes 3−5 Obtained from Voltammograms at 100 mV s^{-1} in DCE Solution Containing 0.1 M $[n\text{-}Bu_4N^+][PF_6^-]$, at 25 ± 2°C[a]

complex	$E_{p,ox}$ ± 5 (mV)	$E_{p,red}$ ± 5 (mV)	$\Delta E = (E_{p,ox} - E_{p,red})$ ± 5 (mV)	$E_{1/2} = 1/2(E_{p,ox} - E_{p,red})$ ± 5 (mV)
2	786	599	187	692
3	718	518	200	618
4	714	563	151	638
5	708	566	142	637

[a]Errors estimated.

of this type recorded in this study. Like the related Fc-C≡C−C≡C-Fc,[32] the bond length data for **2** suggest significant delocalization of π-electron density between the organometallic and heterocyclic units across the alkyne (Table 4); this is further supported by the coplanarity of C_5H_4 and NC_5H_4 rings [max deviation from planarity across both rings = 0.137 Å for C(7); angle between planes C(6)−C(10) and C(13)−C(16)N = 10.55(11)°]. The lattice structure of **2** shows a supramolecular arrangement in which adjacent molecules are linked into dimers by weak C(3)−H(3)···N(1) hydrogen bonds [H(3)··N(1): 2.588(3) Å; ∠C(3)−H(3)···N(1): 169.34(17)°].

Ligand **2** reacts with CuX to form $L_4(CuI)_4$ (**3**), $L_4(CuBr)_2$ (**4**), and $L_4(CuCl)_2$ (**5**). The structures of both **3** and **4** have been determined crystallographically. The structure of the bromide adduct $L_4(CuBr)_2$ (**4**) is dimeric (Figure 3) with copper tetrahedrally coordinated and structurally broadly similar to other $[CuX(N\text{-donor})_2]_2$dimers.[65,66] However, in comparison with $[CuBr(2\text{-}MeC_5H_4N)_2]_2$ the Cu···Cu separation is remarkably short [**4**: 2.620(3) vs 3.351(3) Å] and, to accommodate this, ∠Cu−Br−Cu [**4**: 59.79(5), 60.09(5) vs 80.45(6)°] is extremely acute;[65] the Cu−N bonds are, however, unaffected within experimental error (Table 4). In three of the four pyridyl ligands the heterocycle and one Cp ring are essentially coplanar [angle between C_5H_4 and C_5H_4 N planes: 1.3° for the ligand based on Fe(1), 8.2 °Fe(2), 0.1 °Fe(4)], with only the ligand based on Fe(3) showing a marked twist between planes (24.4°). Any impact this might have on conjugation between the Fc and Cu is masked by the relatively large esds associated with the C−C bonds, and any suggested increase in conjugation here compared to **2** (longer C≡C) is mitigated by Fe−C(≡C) and (C≡)C−C(py) which are at least as long as in **2** (Table 4). As the data for the twisted ligand based on Fe(3) are similar to the remaining three ligands, it would appear that intermolecular interactions in the solid-state, rather than electronic, effects are responsible for any variations in the metric data.

In contrast to the reaction with CuBr, **2** reacts with CuI to form the tetramer $[CuI(L)]_4$ (**3**) (Figure 4). The structure can be thought of as derived from **4**, with loss of **2** allowing two $[CuIL]_2$ to join cofacially via symmetry operation $1 - x, y, {}^1/_2 - z$, with one Cu_2I_2 rotated about 90° with respect to the other while maintaining a coordination number of four at the metal. This, however, brings severe distortions to the Cu_2I_2 ring in comparison with, for example, the Cu_2I_2 ring in dimeric $[CuI(2\text{-}MeC_5H_4N)_2]_2$,[65] becoming elongated between halogens [I(1)··I(2): 4.4549(4) Å (**3**) vs 4.407(3) Å] and compressed between metals [Cu(1)···Cu(2): 2.7084(9) (**3**) vs 3.083(3) Å], and the bond angle at iodine decreasing markedly [Cu(1)−I−Cu(2: 60.998(17), 59.405(16) (**3**) vs 69.95(6) °]. The structure can alternatively be viewed as a compressed Cu_4 tetrahedron with each face capped by a μ_3-iodine. Such arrangements have been noted by others, for example, $[(BzMe_2N)CuI]_4$[67] and $[[(CH_2{=}CH)C_5H_4FeC_5H_4)Ph_2P]CuI]_4$.[69] Cu−I and Cu−N bonds in **3** are comparable with the average data across a range of $Cu_4I_4(py)_4$ compounds [2.040 (Cu−N), 2.696 (Cu−I)],[41] but the Cu−N bonds are notably shorter in **3** than in either of the two specific examples cited (Table 4). The Cu···Cu separations in **3** lie in the range 2.5659(11)−2.7093(9) Å, which are at the shorter end of the range observed in similar systems (2.602−3.010; average 2.710 Å)[68] and includes the shortest such separations seen to date in $Cu_4I_4L_4$ (L = 2e N-donor) systems. The loss of coplanarity between C_5H_4 and NC_5H_4 rings evident to a limited degree in **4** occurs again and more markedly in **3** [angle between planes C(6)−C(10) and C(13)−N(1) 23.8(2); C(26)−C(30) and C(33)−N(2) 15.96(18)°]. In comparison with **2**, features within the alkyne are suggestive of a more localized C≡C and reduced delocalization between Fc and Cu (Table 4).

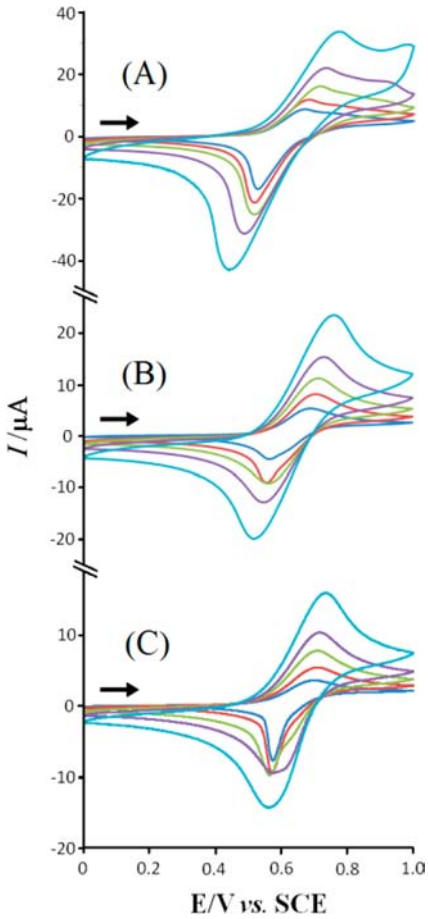

Figure 5. Cyclic voltammograms (scan rates 20, 50, 100, 200, and 500 mV s^{-1}) for ca. 1 mM solution of complexes **3**, **4**, and **5** as (A), (B), and (C), respectively, in DCE with 0.1 M $[n\text{-}Bu_4N^+][PF_6^-]$ as supporting electrolyte at 25 ± 2 °C.

Electrochemistry. Cyclic voltammograms for the oxidation of **2** and for complexes **3**−**5** were obtained from about 1 mM solutions in dichloroethane (DCE) with 0.1 M $[n\text{-}Bu_4N^+][PF_6^-]$

dx.doi.org/10.1021/ic401803p | Inorg. Chem. 2013, 52, 12012−12022

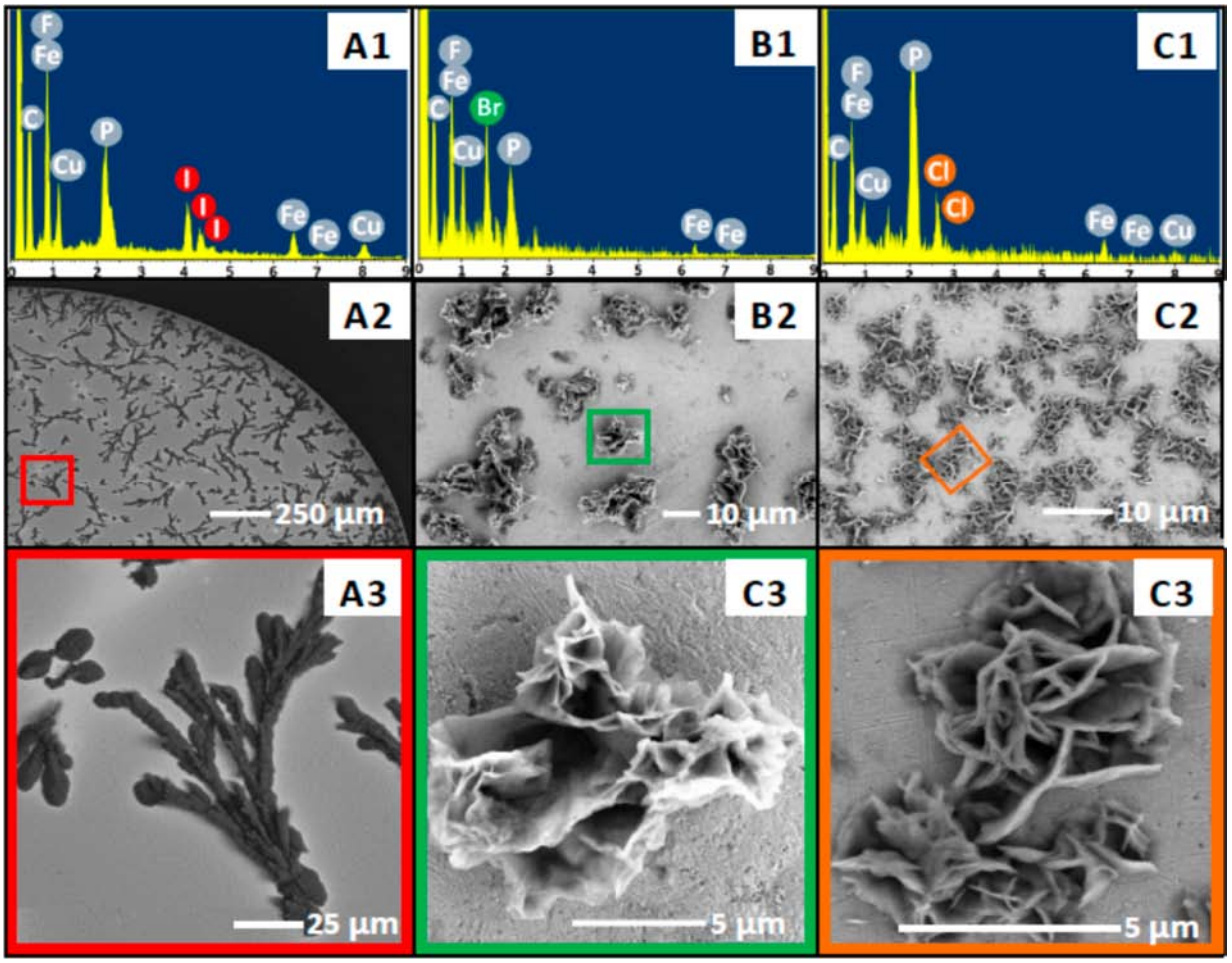

Figure 6. EDX spectra and SEM images of electro-crystallized products $[\mathbf{3}^{4+}][PF_6^-]_4$, $[\mathbf{4}^{2+}][PF_6^-]_2$, and $[\mathbf{5}^{4+}][PF_6^-]_4$ from oxidation of 1 mM solution in DCE for complexes **3**, **4**, and **5** in the presence of 0.1 M $[n\text{-}Bu_4N^+][PF_6^-]$ (electrodeposition for 300 s at +0.9 V). Panels: (A1), (B1), and (C1) show EDX spectra; (A2), (B2), and (C2) show low magnification, and (A3), (B3), and (C3)show high-magnification SEM images of $[\mathbf{3}^{4+}][PF_6^-]_4$, $[\mathbf{4}^{2+}][PF_6^-]_2$, and $[\mathbf{5}^{4+}][PF_6^-]_4$, respectively.

Table 6. EDX Results for Electro-Crystallized $[\mathbf{3}^{4+}][PF_6^-]_4$, $[\mathbf{4}^{2+}][PF_6^-]_2$, and $[\mathbf{5}^{4+}][PF_6^-]_4$ from Oxidation of Complexes 3, 4, and 5 (see Figure 6)[a]

	Fe: Cu	Fe:P	P:F	Cu:X
$[\mathbf{3}]^{4+}[PF_6^-]_4$ or $[L_4(CuI)_4]^{4+}[PF_6^-]_4$	1: 1.0	1: 1.1	1: 6.9	1:1.1 (X = I)
$[\mathbf{4}]^{2+}[PF_6^-]_2$ or $[L_4(CuBr)_2]^{2+}[PF_6^-]_2$	2: 1.1	2: 1.0	1: 5.2	1:1.0 (X = Br)
$[\mathbf{5}]^{4+}[PF_6^-]_4$ or $[L_4(CuCl)_2]^{4+}[PF_6^-]_4$	2: 1.4	1: 1.2	1: 5.2	1:1.5 (X = Cl)

[a]Key elemental ratios are given.

as supporting electrolyte at room temperature (see Figure 5). Data were recorded vs SCE as a function of scan rate (20−1000 mV s^{-1}). The cyclic voltammogram for **2** showed a single reversible redox system with midpoint potential $E_{1/2}$ at 692 mV [here $E_{1/2} = 1/2(E_{p,ox} + E_{p,red})$]. The cyclic voltammograms for complexes **3**−**5** all exhibited unresolved reversible multielectron redox peaks of more complex shape (vide infra). Midpoint potential ($E_{1/2}$) values ranged from 618 mV to 638 mV for the current series of complexes, which are shifted positive compared to standard ferrocene $E_{1/2}$ = 527 mV vs SCE. The shift to more positive $E_{1/2}$ is expected for electron-withdrawing ethynylferrocene complexes[64] (Table 5). The oxidation peak for complexes **3**−**5** were observed to be broadened as compared to that for the ligand **2** (only in part because of uncompensated *iR*-drop). Similar peak broadening, also due to interacting ferrocenylgroups,[33,70−72] has been reported previously. Perhaps surprisingly, at slower scan rates the broad oxidation peaks were associated with a very narrow "stripping" reduction peak, visible in particular at the lowest scan rates[73] (see Figure 5).

The sharp stripping reduction peak is indicative of electrocrystallization of the oxidation product followed by cathodic "stripping".[74] To attempt isolation of the oxidation product, the 3 mm Pt disc working electrode immersed in about 1 mM DCE solution of complex **3** in the presence of 0.1 M $[n\text{-}Bu_4N^+][PF_6^-]$ was held at a constant potential of 900 mV for 300 s. The color of the solution close to the working electrode became darker with time and the formation of a crystalline deposit on the electrode surface was observed. The electrode was removed from solution with potential applied, washed with a few drops of DCE, and the product remaining on the electrode surface was dried under vacuum for 12 h. The crystalline deposits were analyzed by scanning electron microscopy (SEM) and energy-dispersive

dx.doi.org/10.1021/ic401803p | *Inorg. Chem.* 2013, 52, 12012−12022

X-ray analysis (EDX). A similar procedure was followed for electro-deposits of complexes **4** and **5**.

SEM images (Figure 6) of the electro-crystallized product of complex **3** showed denditric growth of the crystals on the electrode surface. The electro-crystallized complex is believed to be the tetra-oxidized complex $\mathbf{3}^{4+}$ stabilized by four $[PF_6]^-$ anions from the supporting electrolyte (tentatively assigned in the absence of direct structural data). This hypothesis is supported by the EDX data showing the Fe:Cu, Cu:I, and Fe:P ratios 1:1.0, 1:1.1, and 1:1.1, respectively, in agreement (within the experimental error of EDX) with the proposed tetramer product complex $[\mathbf{3}^{4+}][PF_6^-]_4$ (Table 6). The dendrite has a structure consisting of a main stem and many side branches.[73] Electrodeposited dendrites have attracted high recent interest for fundamental studies and for potential applications in catalysis and other fields.[43−45,75]

SEM images of the electro-crystallized product of complex **4** show the formation of "lettuce-like" structure on the electrode surface. Each growth is greater than 10 μm. EDX data are consistent with Fe:Cu, Cu:Br, and Fe:P ratios of 2:1.1, 1:1.0, and 2:1.0, respectively, indicative of a complex $[\mathbf{4}^{2+}][PF_6^-]_2$. Formation of this partially oxidized material could be due to a lower solubility of $[\mathbf{4}^{2+}](PF_6^-)_2$ or a faster nucleation process. For complex **5** the SEM images of the electro-crystallization product show "flower-like" morphology when compared to that of oxidized **4**, that is, "lettuce-like", but the growth is spread over less than 10 μm. EDX data imply Fe:Cu, Cu:Cl, and Fe:P ratios of 2:1.4, 1:1.5, and 1:1.2, respectively. The dominating product is likely to be the tetra-oxidized complex $[\mathbf{5}^{4+}][PF_6^-]_4$. The EDX stoichiometries have to be considered as approximate.

The formation of different shapes during crystal growth has been recently demonstrated by Noorduin et al.[76] and explained based on two different growth types: (i) toward the solution and (ii) away from the solution. In our system we noticed both behaviors; dioxidized $[\mathbf{4}^{2+}][PF_6^-]_2$ is grown more vertically (toward the solution, see Figure 6 [B3]) while the tetra-oxidized $[\mathbf{3}^{4+}][PF_6^-]_4$ and $[\mathbf{5}^{4+}][PF_6^-]_4$ are grown more horizontally (away from the solution see Figure 6 [A3 and C3]) with respect to the electrode surface. The reason for this growth behavior is currently unknown and more work will be necessary to confirm the molecular structure of oxidation products. The observation of partially oxidized materials could be important because of their more unusual electronic properties, which in this case could be expected to be similar to that of a doped material or a material with partially filled Fe d-band.[34,36] The design of complex shapes from simple components with a high level of control over morphology holds promise for applications in optics and in catalysis.[76−78]

CONCLUSION

A series of new tetra-ferrocenyl-ethynylpyridinyl complexes of copper(I) halides has been obtained. These poly nuclear complexes can be oxidized under mild conditions with formation of partially- or fully oxidized electro-crystallization products. The inherent structural features based on aromatic and ethyne as well as metal cluster components potentially provide high electron-mobility and therefore these crystalline materials with partially- and fully occupied ferrocene electronic band structure will be of interest in future electronic materials and in optical components (with IVCT bands in the NIR range). The incorporation of $[PF_6]^-$ into the structure can be considered as a "structurally well-defined" doping with implications for photoexcitation and electronic conductivity.[79,80] Furthermore, a combination of mobile electrons and structural rearrangements, which could be possible in these novel materials, may provide an entry into a new class of multiferroics.[41,81]

ASSOCIATED CONTENT

Supporting Information

Crystallographic data in CIF format. This material is available free of charge via the Internet at http://pubs.acs.org. Crystallographic data for the structural analysis (in CIF format) have been deposited with the Cambridge Crystallographic Data Centre, CCDC nos. 912102−912104 for **2**−**4**, respectively. Copies of this information may be obtained from the Director, CCDC, 12 Union Road, Cambridge, CB21EZ, U.K. (Fax: +44−1233−336033; e-mail: deposit@ccdc.cam.ac.uk or www.ccdc.cam.ac.uk).

AUTHOR INFORMATION

Corresponding Authors

*E-mail: msk@squ.edu.om (M.S.K.).
*E-mail: p.r.raithby@bath.ac.uk (P.R.R.).
*E-mail: k.c.molloy@bath.ac.uk (K.C.M.).
*E-mail: f.marken@bath.ac.uk (F.M.).

Notes

The authors declare no competing financial interest.

ACKNOWLEDGMENTS

M.S.K. acknowledges Sultan Qaboos University for Research Grant IG/SCI/CHEM/13/01 and for a research leave while H.H.S. and R.A.Al-B. acknowledge Sultan Qaboos University, Oman, for Ph.D. scholarships. We are grateful to the British Council for a PMI-2 Grant (GS 216) that has supported M.S.K., M.K.Al-S., H.H.S., P.R.R., and K.C.M. P.R.R. gratefully acknowledges support from the EPSRC through the award of a Senior Fellowship (EP/D072859/1) and C.H.W. for the award of a project studentship (EP/F021151/1). This work was conducted as part of a project submitted to The Research Council (TRC), Oman (ORG/EI/13/010). The authors would like to thank Dr. John Mitchels from the Microscopy and Analysis Suite, University of Bath, for his help in initial SEM and EDX data collection.

REFERENCES

(1) Angamuthu, R.; Byers, P.; Lutz, M.; Spek, A. L.; Bouwman, E. *Science* **2010**, *327*, 313.
(2) Perruchas, S.; Desboeufs, N.; Maron, S.; Le Goff, X. F.; Fargues, A.; Garcia, A.; Gacoin, T.; Boilot, J.-P. *Inorg. Chem.* **2011**, *51*, 794.
(3) Perruchas, S.; Goff, X. F. L.; Maron, S.; Maurin, I.; Guillen, F.; Garcia, A.; Gacoin, T.; Boilot, J.-P. *J. Am. Chem. Soc.* **2010**, *132*, 10967.
(4) Safko, J. P.; Kuperstock, J. E.; McCullough, S. M.; Noviello, A. M.; Li, X.; Killarney, J. P.; Murphy, C.; Patterson, H. H.; Bayse, C. A.; Pike, R. D. *Dalton Trans.* **2012**, *41*, 11663.
(5) Igawa, S.; Hashimoto, M.; Kawata, I.; Yashima, M.; Hoshino, M.; Osawa, M. *J. Mater. Chem. C* **2013**, *1*, 542.
(6) Braga, D.; Grepioni, F.; Maini, L.; Mazzeo, P. P.; Ventura, B. *New J. Chem.* **2011**, *35*, 339.
(7) Pike, R. D.; Reinecke, B. A.; Dellinger, M. E.; Wiles, A. B.; Harper, J. D.; Cole, J. R.; Dendramis, K. A.; Borne, B. D.; Harris, J. L.; Pennington, W. T. *Organometallics* **2004**, *23*, 1986.
(8) Kim, T. H.; Shin, Y. W.; Lee, S. S.; Kim, J. *Inorg. Chem. Commun.* **2007**, *10*, 11.
(9) Kim, T. H.; Shin, Y. W.; Jung, J. H.; Kim, J. S.; Kim, J. *Angew. Chem., Int. Ed.* **2008**, *47*, 685.

(10) Perruchas, S.; Tard, C.; Le Goff, X. F.; Fargues, A.; Garcia, A.; Kahlal, S.; Saillard, J.-Y.; Gacoin, T.; Boilot, J.-P. *Inorg. Chem.* **2011**, *50*, 10682.
(11) Jess, I.; Näther, C. *Inorg. Chem.* **2006**, *45*, 7446.
(12) Näther, C.; Jess, I. *Inorg. Chem.* **2003**, *42*, 2968.
(13) Graham, P. M.; Pike, R. D.; Sabat, M.; Bailey, R. D.; Pennington, W. T. *Inorg. Chem.* **2000**, *39*, 5121.
(14) Näther, C.; Jeß, I. *J. Solid State Chem.* **2002**, *169*, 103.
(15) Kyle, K. R.; Ryu, C. K.; Ford, P. C.; DiBenedetto, J. A. *J. Am. Chem. Soc.* **1991**, *113*, 2954.
(16) Kyle, K. R.; Ford, P. C. *J. Am. Chem. Soc.* **1989**, *111*, 5005.
(17) Vogler, A.; Kunkely, H. *J. Am. Chem. Soc.* **1986**, *108*, 7211.
(18) Ryu, C. K.; Vitale, M.; Ford, P. C. *Inorg. Chem.* **1993**, *32*, 869.
(19) Lai, D. C.; Zink, J. I. *Inorg. Chem.* **1993**, *32*, 2594.
(20) Khan, M. S.; Kakkar, A. K.; Long, N. J.; Lewis, J.; Raithby, P.; Nguyen, P.; Marder, T. B.; Wittmann, F.; Friend, R. H. *J. Mater. Chem.* **1994**, *4*, 1227.
(21) Köhler, A.; Wittmann, H. F.; Friend, R. H.; Khan, M. S.; Lewis, J. *Synth. Met.* **1994**, *67*, 245.
(22) Younus, M.; Köhler, A.; Cron, S.; Chawdhury, N.; Al-Mandhary, M. R. A.; Khan, M. S.; Lewis, J.; Long, N. J.; Friend, R. H.; Raithby, P. R. *Angew. Chem., Int. Ed.* **1998**, *37*, 3036.
(23) Wilson, J. S.; Chawdhury, N.; Al-Mandhary, M. R. A.; Younus, M.; Khan, M. S.; Raithby, P. R.; Köhler, A.; Friend, R. H. *J. Am. Chem. Soc.* **2001**, *123*, 9412.
(24) Wilson, J. S.; Dhoot, A. S.; Seeley, A. J. A. B.; Khan, M. S.; Kohler, A.; Friend, R. H. *Nature* **2001**, *413*, 828.
(25) Kohler, A.; Wilson, J. S.; Friend, R. H.; Al-Suti, M. K.; Khan, M. S.; Gerhard, A.; Bassler, H. *J. Chem. Phys.* **2002**, *116*, 9457.
(26) Khan, M. S.; Al-Suti, M. K.; Al-Mandhary, M. R. A.; Ahrens, B.; Bjernemose, J. K.; Mahon, M. F.; Male, L.; Raithby, P. R.; Friend, R. H.; Kohler, A.; Wilson, J. S. *Dalton Trans.* **2003**, 65.
(27) Khan, M. S.; Al-Mandhary, M. R. A.; Al-Suti, M. K.; Al-Battashi, F. R.; Al-Saadi, S.; Ahrens, B.; Bjernemose, J. K.; Mahon, M. F.; Raithby, P. R.; Younus, M.; Chawdhury, N.; Kohler, A.; Marseglia, E. A.; Tedesco, E.; Feeder, N.; Teat, S. J. *Dalton Trans.* **2004**, 2377.
(28) Li, P.; Ahrens, B.; Feeder, N.; Raithby, P. R.; Teat, S. J.; Khan, M. S. *Dalton Trans.* **2005**, 874.
(29) Sudha Devi, L.; Al-Suti, M. K.; Zhang, N.; Teat, S. J.; Male, L.; Sparkes, H. A.; Raithby, P. R.; Khan, M. S.; Köhler, A. *Macromolecules* **2009**, *42*, 1131.
(30) Khan, M. S.; Al-Suti, M. K.; Shah, H. H.; Al-Humaimi, S.; Al-Battashi, F. R.; Bjernemose, J. K.; Male, L.; Raithby, P. R.; Zhang, N.; Kohler, A.; Warren, J. E. *Dalton Trans.* **2011**, *40*, 10174.
(31) Kohler, A.; Khan, A. L. T.; Wilson, J. S.; Dosche, C.; Al-Suti, M. K.; Shah, H. H.; Khan, M. S. *J. Chem. Phys.* **2012**, *136*, 094905.
(32) Diallo, A. K.; Absalon, C.; Ruiz, J.; Astruc, D. *J. Am. Chem. Soc.* **2011**, *133*, 629.
(33) Shah, H. H.; Al-Balushi, R. A.; Al-Suti, M. K.; Khan, M. S.; Woodall, C. H.; Molloy, K. C.; Raithby, P. R.; Robinson, T. P.; Dale, S. E. C.; Marken, F. *Inorg. Chem.* **2013**, *52*, 4898.
(34) Jiao, J.; Long, G. J.; Rebbouh, L.; Grandjean, F.; Beatty, A. M.; Fehlner, T. P. *J. Am. Chem. Soc.* **2005**, *127*, 17819.
(35) Lent, C. S.; Tougaw, P. D.; Porod, W.; Bernstein, G. H. *Nanotechnology* **1993**, *4*, 49.
(36) Jiao, J.; Long, G. J.; Grandjean, F.; Beatty, A. M.; Fehlner, T. P. *J. Am. Chem. Soc.* **2003**, *125*, 7522.
(37) Ghosh, K.; Hu, J.; White, H. S.; Stang, P. J. *J. Am. Chem. Soc.* **2009**, *131*, 6695.
(38) Kobayashi, K.; Horiuchi, S.; Kumai, R.; Kagawa, F.; Murakami, Y.; Tokura, Y. *Phys. Rev. Lett.* **2012**, *108*, 237601.
(39) Collet, E.; Lemée-Cailleau, M.-H.; Buron-Le Cointe, M.; Cailleau, H.; Wulff, M.; Luty, T.; Koshihara, S.-Y.; Meyer, M.; Toupet, L.; Rabiller, P.; Techert, S. *Science* **2003**, *300*, 612.
(40) Polyakov, A. O.; Arkenbout, A. H.; Baas, J.; Blake, G. R.; Meetsma, A.; Caretta, A.; van Loosdrecht, P. H. M.; Palstra, T. T. M. *Chem. Mater.* **2011**, *24*, 133.
(41) Tayi, A. S.; Shveyd, A. K.; Sue, A. C. H.; Szarko, J. M.; Rolczynski, B. S.; Cao, D.; Kennedy, T. J.; Sarjeant, A. A.; Stern, C. L.; Paxton, W. F.; Wu, W.; Dey, S. K.; Fahrenbach, A. C.; Guest, J. R.; Mohseni, H.; Chen, L. X.; Wang, K. L.; Stoddart, J. F.; Stupp, S. I. *Nature* **2012**, *488*, 485.
(42) Pardo, E.; Train, C.; Liu, H.; Chamoreau, L.-M.; Dkhil, B.; Boubekeur, K.; Lloret, F.; Nakatani, K.; Tokoro, H.; Ohkoshi, S.-i.; Verdaguer, M. *Angew. Chem., Int. Ed.* **2012**, *51*, 8356.
(43) Qiu, R.; Zhang, X. L.; Qiao, R.; Li, Y.; Kim, Y. I.; Kang, Y. S. *Chem. Mater.* **2007**, *19*, 4174.
(44) Shin, H. C.; Liu, M. *Adv. Funct. Mater.* **2005**, *15*, 582.
(45) Siegfried, M. J.; Choi, K.-S. *Angew. Chem., Int. Ed.* **2008**, *47*, 368.
(46) Choo, H.; He, B.; Liew, K. Y.; Liu, H.; Li, J. *J. Mol. Catal. A: Chem* **2006**, *244*, 217.
(47) Luo, S.-J.; Liu, Y.-H.; Liu, C.-M.; Liang, Y.-M.; Ma, Y.-X. *Synth. Commun.* **2000**, *30*, 1569.
(48) Sheldrick, G. M. *Acta Crystallogr., Sect. A* **1990**, *46*, 467.
(49) Sheldrick, G. M. *Acta Crystallogr., Sect. A* **2008**, *64*, 112.
(50) Sun, S.-S.; Tran, D. T.; Odongo, O. S.; Lees, A. J. *Inorg. Chem.* **2001**, *41*, 132.
(51) Chawdhury, N.; Long, N. J.; Mahon, M. F.; Ooi, L.-l.; Raithby, P. R.; Rooke, S.; White, A. J. P.; Williams, D. J.; Younus, M. *J. Organomet. Chem.* **2004**, *689*, 840.
(52) Huang, P.; Jin, B.; Liu, P.; Cheng, L.; Cheng, W.; Zhang, S. *J. Organomet. Chem.* **2012**, *697*, 57.
(53) Thomas, K. R. J.; Lin, J. T.; Wen, Y. S. *Organometallics* **2000**, *19*, 1008.
(54) Loch, J. A.; Albrecht, M.; Peris, E.; Mata, J.; Faller, J. W.; Crabtree, R. H. *Organometallics* **2002**, *21*, 700.
(55) Nishiyama, H.; Yamaguchi, S.; Kondo, M.; Itoh, K. *J. Org. Chem.* **1992**, *57*, 4306.
(56) Mohammadi, N.; Ganesan, A.; Chantler, C. T.; Wang, F. *J. Organomet. Chem.* **2012**, *713*, 51.
(57) Goher, M. A. S.; Mautner, F. A. *Polyhedron* **2000**, *19*, 601.
(58) Mautner, F. A.; Goher, M. A. s. *Polyhedron* **1998**, *18*, 553.
(59) Lawrence, E. J.; Wildgoose, G. G.; Aldous, L.; Wu, Y. A.; Warner, J. H.; Compton, R. G.; McNaughter, P. D. *Chem. Mater.* **2011**, *23*, 3740.
(60) Sarkar, S.; Sampath, S. *Langmuir* **2006**, *22*, 3396.
(61) MacLachlan, M. J.; Zheng, J.; Thieme, K.; Lough, A. J.; Manners, I.; Mordas, C.; LeSuer, R.; Geiger, W. E.; Liable-Sands, L. M.; Rheingold, A. L. *Polyhedron* **2000**, *19*, 275.
(62) Ferrer, M.; Gutiérrez, A.; Rodríguez, L.; Rossell, O.; Lima, J. C.; Font-Bardia, M.; Solans, X. *Eur. J. Inorg. Chem.* **2008**, *2008*, 2899.
(63) Cuffe, L.; Hudson, R. D. A.; Gallagher, J. F.; Jennings, S.; McAdam, C. J.; Connelly, R. B. T.; Manning, A. R.; Robinson, B. H.; Simpson, J. *Organometallics* **2005**, *24*, 2051.
(64) Diallo, A. K.; Daran, J.-C.; Varret, F.; Ruiz, J.; Astruc, D. *Angew. Chem., Int. Ed.* **2009**, *48*, 3141.
(65) Dyason, J. C.; Engelhardt, L. M.; Healy, P. C.; Pakawatchai, C.; White, A. H. *Inorg. Chem.* **1985**, *24*, 1950.
(66) Healy, P. C.; Pakawatchai, C.; Raston, C. L.; Skelton, B. W.; White, A. H. *J. Chem. Soc., Dalton Trans.* **1983**, 1905.
(67) Yang, S.; Li, Y.; Cui, Y.; Pan, J. *Acta Crystallogr. Sect. E* **2009**, *65*, m906.
(68) Vega, A.; Saillard, J.-Y. *Inorg. Chem.* **2004**, *43*, 4012.
(69) Štěpnička, P. *Collect. Czech. Chem. Commun.* **2006**, 71.
(70) Mercs, L.; Neels, A.; Albrecht, M. *Dalton Trans.* **2008**, 5570.
(71) Reddinger, J. L.; Reynolds, J. R. *Macromolecules* **1997**, *30*, 673.
(72) Plenio, H.; Hermann, J.; Sehring, A. *Chem.—Eur. J.* **2000**, *6*, 1820.
(73) Engelman, E. E.; Evans, D. H. *J. Electroanal. Chem.* **1993**, *349*, 141.
(74) Qiu, F.; Compton, R. G.; Marken, F.; Wilkins, S. J.; Goeting, C. H.; Foord, J. S. *Anal. Chem.* **2000**, *72*, 2362.
(75) Galenko, P. K.; Zhuravlev, V. A *Physics of Dendrites*; World Scientific: Singapore, 1994.
(76) Noorduin, W. L.; Grinthal, A.; Mahadevan, L.; Aizenberg, J. *Science* **2013**, *340*, 832.
(77) Vlieg, E. *Science* **2013**, *340*, 822.
(78) Zhai, Y.; Pierre, D.; Si, R.; Deng, W.; Ferrin, P.; Nilekar, A. U.; Peng, G.; Herron, J. A.; Bell, D. C.; Saltsburg, H.; Mavrikakis, M.; Flytzani-Stephanopoulos, M. *Science* **2010**, *329*, 1633.

(79) Gao, M.; Lu, C.; Jean-Ruel, H.; Liu, L. C.; Marx, A.; Onda, K.; Koshihara, S.-y.; Nakano, Y.; Shao, X.; Hiramatsu, T.; Saito, G.; Yamochi, H.; Cooney, R. R.; Moriena, G.; Sciaini, G.; Miller, R. J. D. *Nature* **2013**, *496*, 343.
(80) Jérome, D. *Science* **1991**, *252*, 1509.
(81) Horiuchi, S.; Tokunaga, Y.; Giovannetti, G.; Picozzi, S.; Itoh, H.; Shimano, R.; Kumai, R.; Tokura, Y. *Nature* **2010**, *463*, 789.